arXiv:1606.01804v1 [physics.ins-det] 6 Jun 2016

An ultracold neutron storage bottle for UCN density measurements

G. Bison[a], F. Burri[a], M. Daum[a], K. Kirch[a,b], J. Krempel[b], B. Lauss[a,*], M. Meier[a], D. Ries[a,b,**], P. Schmidt-Wellenburg[a], G. Zsigmond[a]

[a] *Paul Scherrer Institute (PSI), CH-5232 Villigen PSI, Switzerland*
[b] *Institute for Particle Physics, Eidgenössische Technische Hochschule (ETH), Zürich, Switzerland*

Abstract

We have developed a storage bottle for ultracold neutrons (UCN) in order to measure the UCN density at the beamports of the Paul Scherrer Institute's (PSI) UCN source. This paper describes the design, construction and commissioning of the robust and mobile storage bottle with a volume comparable to typical storage experiments (32 L) e.g. searching for an electric dipole moment of the neutron.

Keywords: ultracold neutron, neutron storage, neutron density, ultracold neutron source

PACS: 28.20.Gd,28.20.-v,29.25.Dz,61.80.Hg

1. Introduction

Ultracold neutrons (UCN) are neutrons with kinetic energies below about 350 neV, corresponding to a temperature of about 4 mK. Such neutrons are reflected under all angles of incidence from surfaces of suitable materials. Therefore, UCN can be confined in material containers, dubbed 'storage bottles', in which storage times of several hundreds of seconds are possible and ultimately limited by the neutron beta-decay lifetime of 880 s. This unique feature makes UCN ideal to study fundamental properties of the neutron in precision experi-

*Corresponding author, bernhard.lauss@psi.ch
**Corresponding author, dieter.ries@psi.ch

ments [1] like most prominently in the search for an electric dipole moment of the neutron (nEDM) [2–6] or the determination of the lifetime of the free neutron [7, 8], the measurement of neutron decay correlations [9–11] or the investigation of neutron states bound in the Earth's gravitational field [12–14].

The precision of such experiments is limited by the number of UCN available to the experiment. Hence, worldwide efforts to provide higher intensities of UCN are under way. In addition to the ILL PF2 facility [15], which has been leading the field during the last 30 years, several new UCN sources are already in operation [16–19].

At the Paul Scherrer Institute (PSI), Villigen, Switzerland a new UCN source was constructed and has been in operation since 2011 [19–22].

One important benchmark parameter for the performance of a UCN source is the available UCN density which can be stored in an external experiment. In order to determine the UCN densities at different beamports or sources in a consistent way, we have constructed a mobile storage vessel.

2. Design and construction of the storage experiment

In a first attempt, using the prestorage vessel from Ref. [23], which is a NiMo-coated glass tube, and two beamline shutters, UCN densities larger than $20\,\mathrm{UCN/cm^3}$ were measured at PSI's West-1 beamport [24]. However, these measurements were limited by UCN shutter actuation times and UCN losses during actuation.

The main goals for a new storage setup were: construction using commercially available stainless steel (SST) tubing, mobility of the setup and hence a necessary certain robustness of construction, fast shutters without unnecessary UCN losses via openings during movement. The overall volume of the setup should be similar to a typical storage vessel employed in a nEDM measurement, i.e. larger than 20 L, and have a Fermi potential (V_F) on the surface well suited for UCN storage. The employed stainless steel alloys have a calculated V_F of about 188 neV. The Fermi potential in the UCN storage chamber of the

currently best nEDM experiment is given by "deuterated polystyrene" used as coating of the electrical insulator (V_F=161 neV [25]).

2.1. UCN shutters

Two butterfly-valve-type shutters with 200 mm opening were designed and built. One is depicted in Fig. 1. All parts inside the storage volume which can be in contact with UCN are made from stainless steel. The shutters can be connected to outer diameter 204 mm standard tubes. The shutter blades (SST type 1.4301) were polished mechanically and are mounted to the rotating axis, such that all screws are mounted from one side, while the other side has a continuous surface. The shutter housing material is SST type 1.4435.

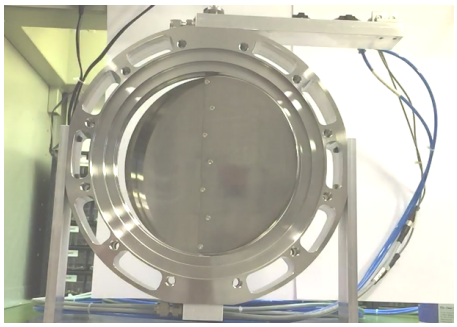

Figure 1: Photograph of one of the shutters. Pressurized air and cables for position indicators are on the right hand side. Cut-outs from the stainless steel body are for weight reduction. The opening for UCN has a diameter of 200 mm.

The shutter disc can be rotated with a pneumatic linear actuator (Festo DSNU-16-50-PPV-A), which delivers a force greater than 100 N along a stroke of 50 mm. An air pressure of about 6 bar is used. The mechanical feedthroughs can be differentially pumped through additional tubes terminated by a KF16 flange. Figure 2 shows a technical drawing of the differentially pumped mechanical feedthrough and actuation mechanism.

On average, the shutter housings add each an average length of 10.0(5) mm to the storage volume of the tube when the shutters are closed.

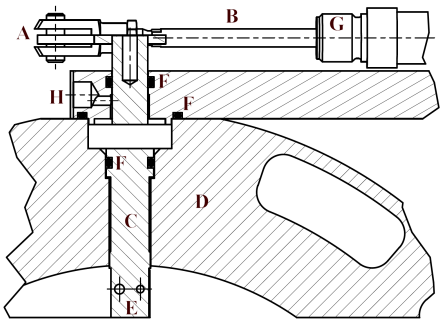

Figure 2: UCN shutter: Technical drawing of the mechanical feedthrough. The pneumatic cylinder is acting on the shutter axis via a lever arm outside the vacuum. The axis feedthrough can be differentially pumped. The holes on the bottom of the axis are used to mount the shutter blades. A: lever arm, B: piston, C: rotation axis, D: frame, E: axis mounting for blades, F: viton sealing, G: pneumatic actuator, H: pump port;

Opening and closing times of less than 100 ms were measured using a series of high speed camera pictures as shown in Fig. 3.

Using a duration t of the movement of 100 ms and a radius r of the bottle of 100 mm, the maximum speed of the outer edge of the shutter blade during movement is $1.57\,\mathrm{m\,s^{-1}}$, which is considerably slower than the UCN velocities in the bottle and hence has only a small influence on the stored UCN density.

2.2. Storage bottle

A 1000.0(5) mm long stainless steel tube, ID=200 mm, OD=204 mm, complying with DIN 11866, with a specified inner surface roughness of $R_\mathrm{a} < 0.8\,\mu\mathrm{m}$, made by Herrli AG in Kerzers, Switzerland, is sandwiched between the two UCN shutters. The tube was electro-polished to obtain the final surface finishing.

Together with the shutters, this results in a cylindrical UCN storage volume of length 1020.0(11) mm, with an inner diameter of 200.0(5) mm, and therefore with a volume of $32\,044(164)\,\mathrm{cm}^3$.

The shutters are mounted in a support structure made from aluminum profiles, which provide a solid, flat pedestal and simplifies handling during assembly.

At the flanges of both shutters 150(1) mm long SST extension tubes are

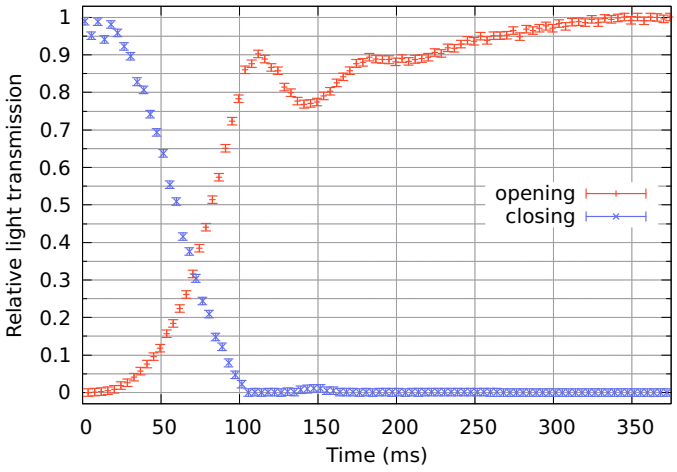

Figure 3: Opening and closing behavior of the UCN shutters measured by comparing the visible white area of the background behind the shutter with the area visible in fully opened position. The movements start at time=0. Closing from fully open to 95 % closed takes less than 100 ms. Opening from zero to 90 % open takes about 120 ms. There is a small swing-back motion caused by the break of the pneumatic cylinder.

attached, which guarantee the free movement of the shutter blades and provide connections to the beamport and the detector. Two sizes of Cascade detectors [1] were used for the measurements. One large area ('big') Cascade UCN detector with 20 cm × 20 cm active area [24] and one with 10 cm × 10 cm active area ('small detector') was employed.

Two KF16 vacuum flanges welded on the extension tubes provide ports for pumping and pressure measurement. The one located upstream has the full opening of ID=16 mm, while the one before the detector has a reduced opening of 2 mm. Figures 4 and 5 show a drawing and a photo of the assembled storage bottle.

[1] CD-T Technology, Hans-Bunte Strasse 8-10, 69123 Heidelberg, Germany

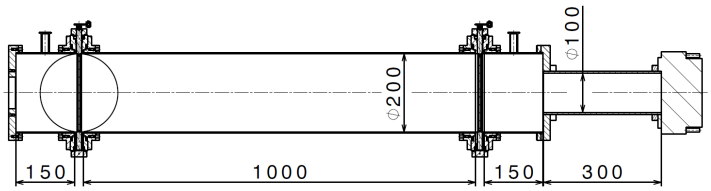

Figure 4: Technical design drawing of the storage experiment. From left to right: connection flange to the beamport, connection guide with KF16 (2 mm) flange, shutter 1, storage bottle, shutter 2, connection guide with KF16 flange, connection flange, 30 cm horizontal extraction guide, small Cascade detector. The big Cascade counter was directly mounted onto the connection guide.

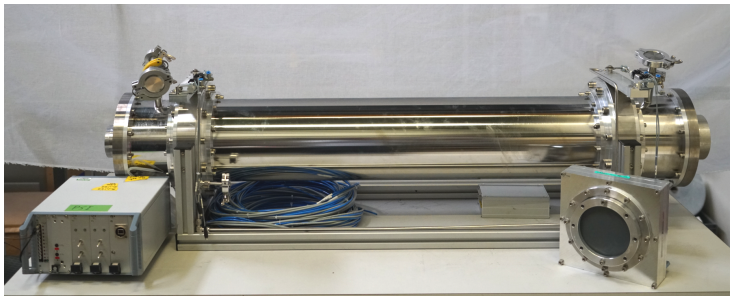

Figure 5: The assembled UCN storage bottle with the small Cascade detector on the right and the timing control unit on the left.

2.3. Timing control

The opening and closing sequence for the two shutters needs to be configurable and reproducible in order to perform UCN storage measurements.

5 V TTL signals are used to control the air flow to the pneumatic actuators. The shutters go into the closed state when no signal (0 V) is present.

In the measurements described here, an Arduino Due board [2] is used for the timing logic. The board is based on a 32-bit micro-controller running at a clock speed of 84 MHz and can be programmed using the C programming language and a hardware abstraction layer provided as open source software. This makes

[2] https://www.arduino.cc/en/Main/ArduinoBoardDue

it very simple to implement a deterministic real-time capable digital controller. Due to the high clock speed, cycle times of 100 µs are easily accomplished.

The program flow is the following:

1. A counter is being increased every 100 µs starting with the rising flank of the trigger input.
2. In the first timing cycle after the trigger, the shutters are set to the filling position, shutter 1 (upstream) open, shutter 2 (downstream) closed.
3. When the counter reaches the predefined filling time, both shutters are set to the closed position, and the storage time is started.
4. When the counter reaches the sum of the predefined filling and storage times, the shutter 2 is opened and the counting period starts.
5. When the counter reaches the sum of the predefined filling, storage and counting times, shutter 1 is opened again and shutter 2 closed; this is the only time when the storage vessel is being vacuum-pumped with open shutter. The counter is reset to zero and the trigger flag is set to false, waiting to be triggered again.

All timing parameters are set through a serial connection from a PC. Manual operation of the two shutters is also possible.

A custom-made 10 channel galvanically-isolated TTL driver card is used to convert the 3.3 V output of the micro-controller board to 5 V. The decoupled 5 V outputs then drive the TTL inputs of the two UCN shutters.

3. Commissioning of the setup

A set of measurements at the West-1 beamport at PSI was performed in fall 2014. The big Cascade UCN detector was used in this measurement. The commissioning measurements were done while the PSI source was operating with a proton beam pulse of only 3.2 s length and a pulse length to repetition time ratio optimized for the nEDM experiment which is mounted at the South beamport. These operating conditions were not well suited for UCN density

measurements at that time, as they had to be done parasitically to nEDM data taking.

3.1. UCN transmission

The UCN transmission of the storage bottle, the shutter, and the connecting tubes was measured by comparing 2 setups. After a first measurement with the detector connected directly to the beamport, the storage bottle was inserted between the detector and the beamport for a second measurement. The transmission is then calculated, similar as done in [23], as the ratio of counts obtained in the two measurements. Measurements in both configurations were repeated several times. Since the UCN source output for different proton pulses fluctuates more than standard counting statistics, the standard deviation of the mean was used as uncertainty.

The proton pulse onto the UCN spallation target in these measurements was always 3.2 s long with a repetition time of 340 s at 2.2 mA beam current. Proton current variations are accounted for in the analysis. UCN were detected continuously, but a delayed time range for counting UCN was chosen with a length of 230 s starting at 10 s after the end of the proton pulse. This guaranteed that only storable UCN were counted, as during the proton pulse also faster neutrons and other background events may have been detected.

With the detector directly mounted to the beamport about 1×10^7 UCN were counted per pulse in the total time range and 7.0×10^6 UCN in the delayed time window; after mounting the storage bottle the respective UCN counts were about 8×10^6 UCN (total window) and 5.7×10^6 UCN (delayed window). Correcting for a small difference in proton beam current between the measurements, this results in a UCN transmission of 81.7(1) % caused by the Fermi potential and surface conditions of the storage bottle and unavoidable small gaps between various UCN guiding parts of the setup.

3.2. UCN leakage

The two shutters are not completely tight with respect to UCN. Comparing the UCN rate in the detector measured with both shutters open to the UCN

rate with one shutter closed, one finds a UCN leakage between 1 % and 2 % for both shutters. Figure 6 shows the measured UCN leakage rates of the two shutters over time.

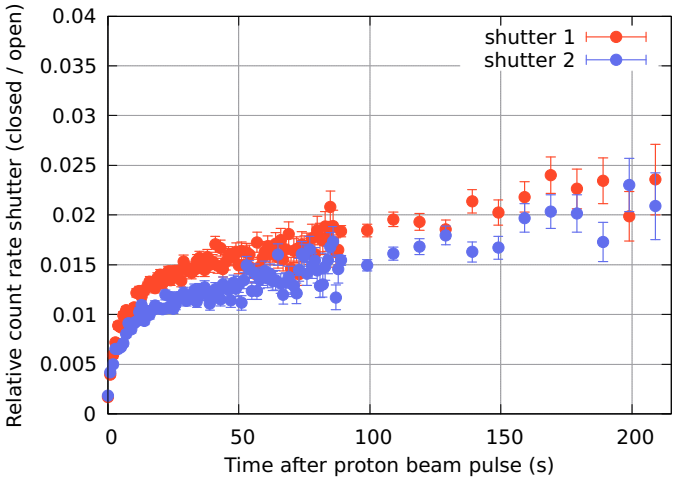

Figure 6: UCN counts (leakage) versus time after the end of the proton pulse. Bin-wise ratio between UCN counts with closed and open shutters. Bins of size 1 s during the first 90 s, bins of size 10 s later. The leakage rate rises quickly from 0 to between 1.0 and 1.5 % after the beginning of UCN production. Afterwards, the leakage rate increases to between 2.0 and 2.5 %, which is simply caused by the shorter emptying time of the source with shutters opened.

Fitting single-exponential decays to the count rates with different shutter positions consistent with [24], results in emptying times of the UCN source of 36.0(3) s for both shutters open and emptying times of 40.0(3) s for shutter 1 closed and 40.8(3) s for shutter 2 closed. This change in emptying time leads to an apparent slow rise of the leakage rate over time. The low leakage rate at short times after the end of the proton pulse is due to the obstruction of the direct UCN flight trajectories to the detector by the closed shutter, which causes a delayed UCN arrival.

3.3. UCN storage

The filling time of the bottle was optimized with 5 s storage measurements. Figure 7 shows the recorded filling time scan with a relatively broad maximum at t=16 s. The timing was started by the proton beam trigger signal at t= 0 which occurs 1 s before the proton beam hits the target. Using the optimized filling time, four measurements with storage times of 2, 5, 25, and 105 seconds and a background measurements with shutter 1 closed were performed.

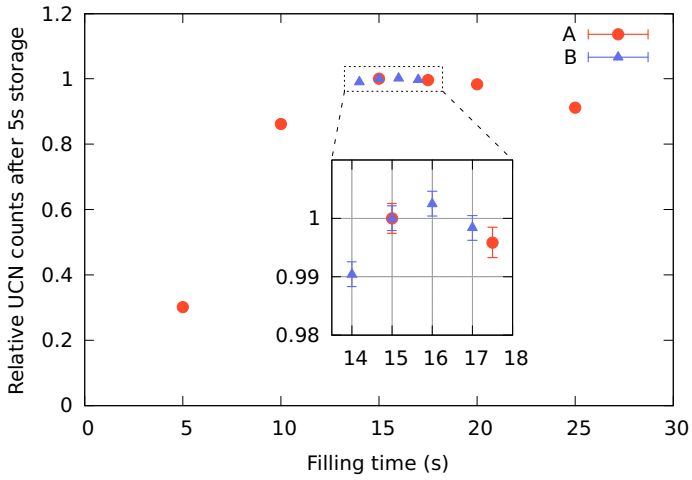

Figure 7: Relative UCN counts measured after 5 s of storage for different filling times. The setup was dismounted between the two performed measurement periods A and B, with a different performance of the UCN source. The measurements are in good agreement. Shown values are normalized to the value at t =15 s measured in period A and B. The best output was measured for t =16 s. Error bars are statistical only and only shown in the zoomed-in area.

The UCN leakage of the shutters made a correction of the measured counts necessary. The UCN counts in the detector were integrated starting from the time when the second shutter was opened until about 260 s after the end of the proton beam pulse. The leakage counts were determined in an measurement which was identical except that shutter 1 stayed closed all the time.

Figure 8 shows an overlay of the measured time spectra in the detector. For

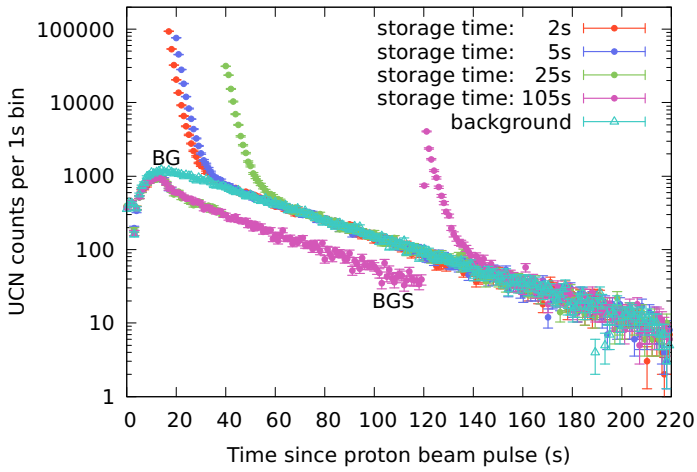

Figure 8: Time spectra of UCN counts in the storage measurement for different storage times using the big Cascade detector. The background curve ('BG') with one shutter closed (open triangles) does not show an emptying peak. The background curve with both shutters closed ('BGS') was measured in the 105 s storage measurement, where shutter 2 opens after this time and the stored UCN are detected in the counting peak.

late times the UCN counts reach again the level of the background.

Figure 9 shows the storage curve together with the fit from the leakage time spectrum using a double-exponential fit function. Tab.1 lists the fit parameters. The storage time constant τ_2 represents the main (slow) UCN component. Statistical errors on the individual points are well below 1 % and are therefore smaller than the symbols in the figure.

Detector	A_1	τ_1(s)	A_2	τ_2(s)	red.χ^2
Big	30(7)	6(5)	56(8)	40(8)	1.13
Small	17(2)	9(2)	52(2)	40(1)	1.23

Table 1: Parameters from the double-exponential fit to the leaking UCN measured with the two Cascade detectors.

Ultracold neutron densities can easily be calculated by dividing the UCN counts after a selected storage time with the total volume of the storage. Be-

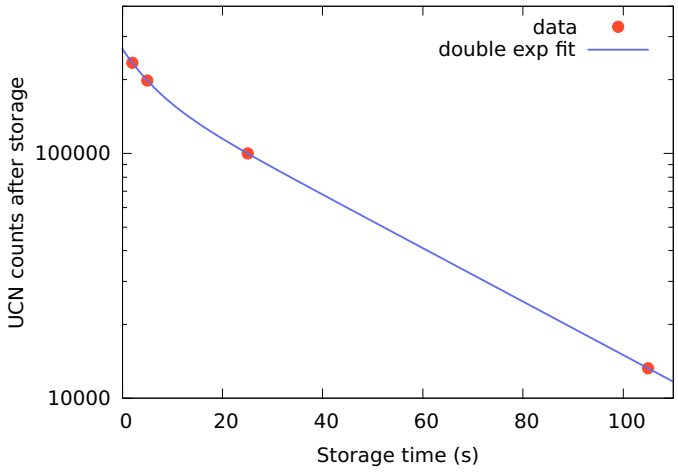

Figure 9: UCN counts in the big Cascade detector after different storage times (symbols) together with the fit function for a double-exponential fits drawn as a line (as given in Tab.1).

cause of the described measurement conditions, mainly due to the short proton pulse length, only half the UCN density compared to previous measurements in Ref. [24] was observed. Dedicated UCN density measurements with the storage bottle described here, will be reported in a forthcoming publication.

3.4. Small detector

The measurements were subsequently repeated and confirmed with the small Cascade detector, which was connected to the bottle using a straight 300 mm piece of NiMo-coated acrylic tube with 100 mm inner diameter. The measured storage curve is shown in Fig. 10. Again, using a double-exponential fit function we obtain the results given in Tab.1. The smaller extraction opening and detector area show no significant influence on the 'relevant' slow component, which represents the UCN storable for longer observation times.

4. Summary

We designed and constructed a storage experiment made from stainless steel components in order to have a mobile and robust setup with fast shutters, to

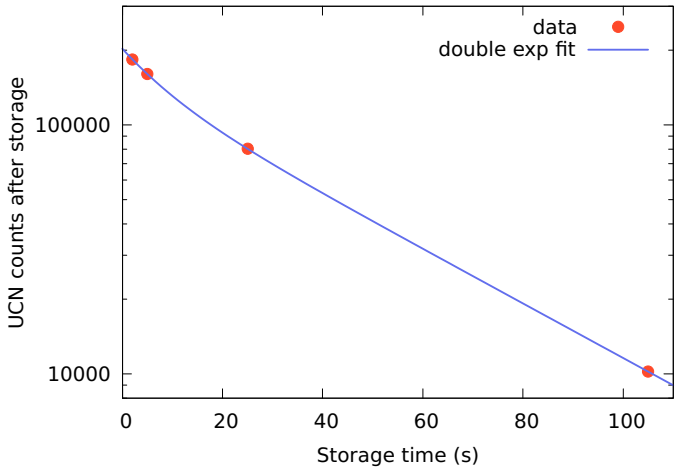

Figure 10: UCN counts in the small Cascade detector after different storage times (symbols) together with the fit function for a double exponential fits drawn as a line (as given in Tab.1).

determine UCN densities at various beamports. The storage bottle was successfully commissioned at the West-1 beamport of the PSI UCN source. The UCN performance characteristics of the storage bottle, namely UCN transmission and storage times were determined for the PSI UCN beam characteristics. Measured integral UCN counts and the known bottle volume can hence be used to derive UCN densities for selected storage times.

5. Acknowledgements

This work is part of the Ph.D. thesis of Dieter Ries. We would like to thank all people who contributed to design and construction of our setup: M. Horisberger, M. Mähr and the AMI shop, M. Müller and his workshop, as well as P. Rüttimann. Support by the Swiss National Science Foundation Projects 200020_137664 and 200020_149813 is gratefully acknowledged.

References

[1] R. Golub, D. Richardson, S. Lamoreaux, Ultra-Cold Neutrons, Adam Hilger, Bristol, Philadelphia, and New York, 1991.

[2] N. F. Ramsey, Electric-dipole moments of particles, Annual Review of Nuclear and Particle Science 32 (1) (1982) 211–233.

[3] C. A. Baker, D. D. Doyle, P. Geltenbort, K. Green, M. G. D. van der Grinten, P. G. Harris, P. Iaydjiev, S. N. Ivanov, D. J. R. May, J. M. Pendlebury, J. D. Richardson, D. Shiers, K. F. Smith, Improved experimental limit on the electric dipole moment of the neutron, Phys. Rev. Lett. 97 (13) (2006) 131801.

[4] C. Baker, G. Ban, K. Bodek, M. Burghoff, Z. Chowdhuri, M. Daum, M. Fertl, B. Franke, P. Geltenbort, K. Green, M. van der Grinten, E. Gutsmiedl, P. Harris, R. Henneck, P. Iaydjiev, S. Ivanov, N. Khomutov, M. Kasprzak, K. Kirch, S. Kistryn, S. Knappe-Gruneberg, A. Knecht, P. Knowles, A. Kozela, B. Lauss, T. Lefort, Y. Lemiere, O. Naviliat-Cuncic, J. Pendlebury, E. Pierre, F. Piegsa, G. Pignol, G. Quemener, S. Roccia, P. Schmidt-Wellenburg, D. Shiers, K. Smith, A. Schnabel, L. Trahms, A. Weis, J. Zejma, J. Zenner, G. Zsigmond, The search for the neutron electric dipole moment at the Paul Scherrer Institute, Physics Procedia 17 (0) (2011) 159 – 167, 2nd International Workshop on the Physics of fundamental Symmetries and Interactions - PSI2010.

[5] A. P. Serebrov, E. A. Kolomenskiy, A. N. Pirozhkov, I. A. Krasnoschekova, A. V. Vassiljev, A. O. Polyushkin, M. S. Lasakov, A. N. Murashkin, V. A. Solovey, A. K. Fomin, I. V. Shoka, O. M. Zherebtsov, P. Geltenbort, S. N. Ivanov, O. Zimmer, E. B. Alexandrov, S. P. Dmitriev, N. A. Dovator, New search for the neutron electric dipole moment with ultracold neutrons at ILL, Phys. Rev. C 92 (2015) 055501.

[6] J. M. Pendlebury, S. Afach, N. J. Ayres, C. A. Baker, G. Ban, G. Bison, K. Bodek, M. Burghoff, P. Geltenbort, K. Green, W. C. Griffith,

M. van der Grinten, Z. D. Grujić, P. G. Harris, V. Hélaine, P. Iaydjiev, S. N. Ivanov, M. Kasprzak, Y. Kermaidic, K. Kirch, H.-C. Koch, S. Komposch, A. Kozela, J. Krempel, B. Lauss, T. Lefort, Y. Lemière, D. J. R. May, M. Musgrave, O. Naviliat-Cuncic, F. M. Piegsa, G. Pignol, P. N. Prashanth, G. Quéméner, M. Rawlik, D. Rebreyend, J. D. Richardson, D. Ries, S. Roccia, D. Rozpedzik, A. Schnabel, P. Schmidt-Wellenburg, N. Severijns, D. Shiers, J. A. Thorne, A. Weis, O. J. Winston, E. Wursten, J. Zejma, G. Zsigmond, Revised experimental upper limit on the electric dipole moment of the neutron, Phys. Rev. D 92 (2015) 092003.

[7] A. Serebrov, V. Varlamov, A. Kharitonov, A. Fomin, Y. Pokotilovski, P. Geltenbort, J. Butterworth, I. Krasnoschekova, M. Lasakov, R. Tal'daev, A. Vassiljev, O. Zherebtsov, Measurement of the neutron lifetime using a gravitational trap and a low-temperature Fomblin coating, Physics Letters B 605 (2005) 72–78.

[8] F. Wietfeldt, G. Greene, The neutron lifetime, Rev. of Modern Physics 83 (2011) 1173–1192.

[9] J. Liu, M. P. Mendenhall, A. T. Holley, H. O. Back, T. J. Bowles, L. J. Broussard, R. Carr, S. Clayton, S. Currie, B. W. Filippone, A. Garcia, P. Geltenbort, K. P. Hickerson, J. Hoagland, G. E. Hogan, B. Hona, T. M. Ito, C.-Y. Liu, M. Makela, R. R. Mammei, J. W. Martin, D. Melconian, C. L. Morris, R. W. Pattie, A. Pérez Galvan, M. L. Pitt, B. Plaster, J. C. Ramsey, R. Rios, R. Russell, A. Saunders, S. J. Seestrom, W. E. Sondheim, E. Tatar, R. B. Vogelaar, B. VornDick, C. Wrede, H. Yan, A. R. Young, Determination of the axial-vector weak coupling constant with ultracold neutrons, Phys. Rev. Lett. 105 (2010) 181803.

[10] B. Plaster, R. Rios, H. O. Back, T. J. Bowles, L. J. Broussard, R. Carr, S. Clayton, S. Currie, B. W. Filippone, A. García, P. Geltenbort, K. P. Hickerson, J. Hoagland, G. E. Hogan, B. Hona, A. T. Holley, T. M. Ito, C.-Y. Liu, J. Liu, M. Makela, R. R. Mammei, J. W. Martin, D. Mel-

conian, M. P. Mendenhall, C. L. Morris, R. Mortensen, R. W. Pattie, A. Pérez Galván, M. L. Pitt, J. C. Ramsey, R. Russell, A. Saunders, R. Schmid, S. J. Seestrom, S. Sjue, W. E. Sondheim, E. Tatar, B. Tipton, R. B. Vogelaar, B. VornDick, C. Wrede, Y. P. Xu, H. Yan, A. R. Young, J. Yuan, Measurement of the neutron β-asymmetry parameter A_0 with ultracold neutrons, Phys. Rev. C 86 (2012) 055501.

[11] M. P. Mendenhall, R. W. Pattie, Y. Bagdasarova, D. B. Berguno, L. J. Broussard, R. Carr, S. Currie, X. Ding, B. W. Filippone, A. García, P. Geltenbort, K. P. Hickerson, J. Hoagland, A. T. Holley, R. Hong, T. M. Ito, A. Knecht, C.-Y. Liu, J. L. Liu, M. Makela, R. R. Mammei, J. W. Martin, D. Melconian, S. D. Moore, C. L. Morris, A. Pérez Galván, R. Picker, M. L. Pitt, B. Plaster, J. C. Ramsey, R. Rios, A. Saunders, S. J. Seestrom, E. I. Sharapov, W. E. Sondheim, E. Tatar, R. B. Vogelaar, B. VornDick, C. Wrede, A. R. Young, B. A. Zeck, Precision measurement of the neutron β-decay asymmetry, Phys. Rev. C 87 (2013) 032501.

[12] V. V. Nesvizhevsky, H. G. Borner, A. K. Petukhov, H. Abele, S. Baeszler, F. J. Ruesz, T. Stoferle, A. Westphal, A. M. Gagarski, G. A. Petrov, A. V. Strelkov, Quantum states of neutrons in the earth's gravitational field, Nature 415 (6869) (2002) 297–299.

[13] T. Jenke, P. Geltenbort, H. Lemmel, H. Abele, Realization of a gravity-resonance-spectroscopy technique, Nature Physics 7 (6) (2011) 468–472.

[14] T. Jenke, G. Cronenberg, J. Burgdörfer, A. Chizhova, L., P. Geltenbort, N. Ivanov, A., T. Lauer, T. Lins, S. Rotter, H. Saul, U. Schmidt, H. Abele, Gravity resonance spectroscopy constrains dark energy and dark matter scenarios, Phys. Rev. Lett. 112 (2014) 151105.

[15] A. Steyerl, H. Nagel, F.-X. Schreiber, K.-A. Steinhauser, R. Gaehler, W. Glaeser, P. Ageron, J. Astruc, W. Drexel, G. Gervais, W. Mampe, A new source of cold and ultracold neutrons, Physics Letters A 116 (7) (1986) 347 – 352.

[16] A. Saunders, M. Makela, Y. Bagdasarova, H. O. Back, J. Boissevain, L. J. Broussard, T. J. Bowles, R. Carr, S. A. Currie, B. Filippone, A. Garcia, P. Geltenbort, K. P. Hickerson, R. E. Hill, J. Hoagland, S. Hoedl, A. T. Holley, G. Hogan, T. M. Ito, S. Lamoreaux, C.-Y. Liu, J. Liu, R. R. Mammei, J. Martin, D. Melconian, M. P. Mendenhall, C. L. Morris, R. N. Mortensen, R. W. Pattie, M. Pitt, B. Plaster, J. Ramsey, R. Rios, A. Sallaska, S. J. Seestrom, E. I. Sharapov, S. Sjue, W. E. Sondheim, W. Teasdale, A. R. Young, B. VornDick, R. B. Vogelaar, Z. Wang, Y. Xu, Performance of the los alamos national laboratory spallation-driven solid-deuterium ultra-cold neutron source, Review of Scientific Instruments 84 (1).

[17] F. M. Piegsa, M. Fertl, S. N. Ivanov, M. Kreuz, K. K. H. Leung, P. Schmidt-Wellenburg, T. Soldner, O. Zimmer, New source for ultracold neutrons at the Institut Laue-Langevin, Phys. Rev. C 90 (2014) 015501.

[18] A. Frei, Y. Sobolev, I. Altarev, K. Eberhardt, A. Gschrey, E. Gutsmiedl, R. Hackl, G. Hampel, F. J. Hartmann, W. Heil, J. V. Kratz, T. Lauer, A. Lion Aguilar, A. R. Mueller, S. Paul, Y. Pokotilovski, W. Schmid, L. Tassini, D. Tortorella, N. Trautmann, U. Trinks, N. Wiehl, First production of ultracold neutrons with a solid deuterium source at the pulsed reactor TRIGA mainz, Eur. Phys. J. A 34 (2) (2007) 119–127.

[19] B. Lauss, Ultracold Neutron Production at the Second Spallation Target of the Paul Scherrer Institute, Physics Procedia 51 (2014) 98.

[20] A. Anghel, F. Atchison, B. Blau, B. van den Brandt, M. Daum, R. Doelling, M. Dubs, P.-A. Duperrex, A. Fuchs, D. George, L. Göltl, P. Hautle, G. Heidenreich, F. Heinrich, R. Henneck, S. Heule, T. Hofmann, S. Joray, M. Kasprzak, K. Kirch, A. Knecht, J. Konter, T. Korhonen, M. Kuzniak, B. Lauss, A. Mezger, A. Mtchedlishvili, G. Petzoldt, A. Pichlmaier, D. Reggiani, R. Reiser, U. Rohrer, M. Seidel, H. Spitzer, K. Thomsen, W. Wagner, M. Wohlmuther, G. Zsigmond, J. Zuellig, K. Bodek, S. Kistryn, J. Zejma, P. Geltenbort, C. Plonka, S. Grigoriev, The PSI ultra-cold neutron source,

Nuclear Instruments and Methods in Physics Research Section A 611 (2009) 272–275.

[21] B. Lauss, A new facility for fundamental particle physics: The high-intensity ultracold neutron source at the Paul Scherrer Institute, AIP Conference Proceedings 1441 (1) (2012) 576–578.

[22] B. Lauss, Startup of the high-intensity ultracold neutron source at the Paul Scherrer Institute, Hyperfine Interactions 211 (2012) 21–25.

[23] B. Blau, M. Daum, M. Fertl, P. Geltenbort, L. Goeltl, R. Henneck, K. Kirch, A. Knecht, B. Lauss, P. Schmidt-Wellenburg, G. Zsigmond, A prestorage method to measure neutron transmission of ultracold neutron guides, Nuclear Instruments and Methods in Physics Research Section A: Accelerators, Spectrometers, Detectors and Associated Equipment 807 (2016) 30 – 40.

[24] L. Göltl, Characterization of the PSI ultra-cold neutron source, Ph.D. thesis, ETH Zürich, No.20350 (2012).

[25] K. Bodek, M. Daum, R. Henneck, S. Heule, M. Kasprzak, K. Kirch, A. Knecht, M. Kuźniak, B. Lauss, M. Meier, G. Petzoldt, M. Schneider, G. Zsigmond, Storage of ultracold neutrons in high resistivity, non-magnetic materials with high Fermi potential, Nuclear Instruments and Methods in Physics Research A 597 (2008) 222–226.